Ultra-Wide Field OCT of Posterior Staphyloma

5

Kosei Shinohara

Abstract

Ultra-wide field OCT (UWF-OCT) is a useful instrument for the detection and classification of posterior staphylomas. Morphological features of posterior staphylomas shown by UWF-OCT are gradual thinning of the choroid from the periphery toward the edge of the staphyloma and a gradual re-thickening of the choroid in the direction toward the posterior pole along with a posterior displacement of the sclera in the staphylomatous area. Also, there is a gradual thickening and inward protrusion of the sclera at the staphyloma edge. UWF-OCT will be a standard instrument for the detection of posterior staphylomas.

Keywords

Posterior staphyloma · Ultra-wide field OCT · Sclera · Choroid

It had long been difficult to visualize the entire extent of posterior staphylomas with conventional optical coherence tomography (OCT) because staphylomas are usually wider than the scanned area by OCT. Therefore, the usefulness of conventional OCT for the detection of staphylomas has been limited to peripapillary staphyloma [1]. As approaches to cover a large area by OCT, combining multiple scans at different locations or placing a +20 diopter lens between the eye and the OCT device were performed. In addition to the limited width of OCT images, the depth of images was not sufficient to accommodate a deep staphyloma [2, 3]. Recent advance in OCT technology has allowed clinicians to evaluate a much wider area than the posterior fundus. Morphological hallmarks of posterior staphylomas as examined by UWF-OCT are; a gradual thinning of the choroid from the periphery toward the staphyloma edges and a gradual re-thickening of the choroid in a direction toward the posterior pole along with a posterior displacement of the sclera in the staphylomatous area (Fig. 5.1). Additionally, there was a gradual thickening and inward protrusion of the sclera at the staphyloma edge (Figs. 5.1, 5.2, 5.3, and 5.4). These features should be used as the criteria of the diagnoses of a posterior staphyloma. Among these morphological changes, the choroidal thinning and the posterior displacement of the sclera are occasionally observed even in children with high myopia (Fig. 5.5), indicating these two features are the early change in the process of the development of staphylomas [4]. Shinohara et al. reported the usefulness of ultra-wide field OCT (UWF-OCT) for the detection of posterior staphylomas compared its usefulness with 3D MRI (Table 5.1) [5].

The advantages of UWF-OCT is that it enables to visualize different tissues such as vitreous, retina, choroid, and sclera in a high resolution. Especially, the spatial relationship between a posterior staphyloma and other tissues such as optic nerve, and retinal vasculature is clearly seen. Due to these advantages, UWF-OCT can detect and classify posterior staphylomas more accurately and objectively than conventional methods, and some subtle staphylomas which are difficult to be detected ophthalmoscopically or by 3D MRI can be detected by UWF-OCT (Fig. 5.6). It is expected that UWF-OCT will be a standard instrument for the detection of posterior staphylomas.

K. Shinohara (✉)
Department of Ophthalmology and Visual Science, Tokyo Medical and Dental University, Tokyo, Japan

Musashino Red-Cross Hospital, Tokyo, Japan

K. Ohno-Matsui (ed.), *Atlas of Pathologic Myopia*, https://doi.org/10.1007/978-981-15-4261-9_5

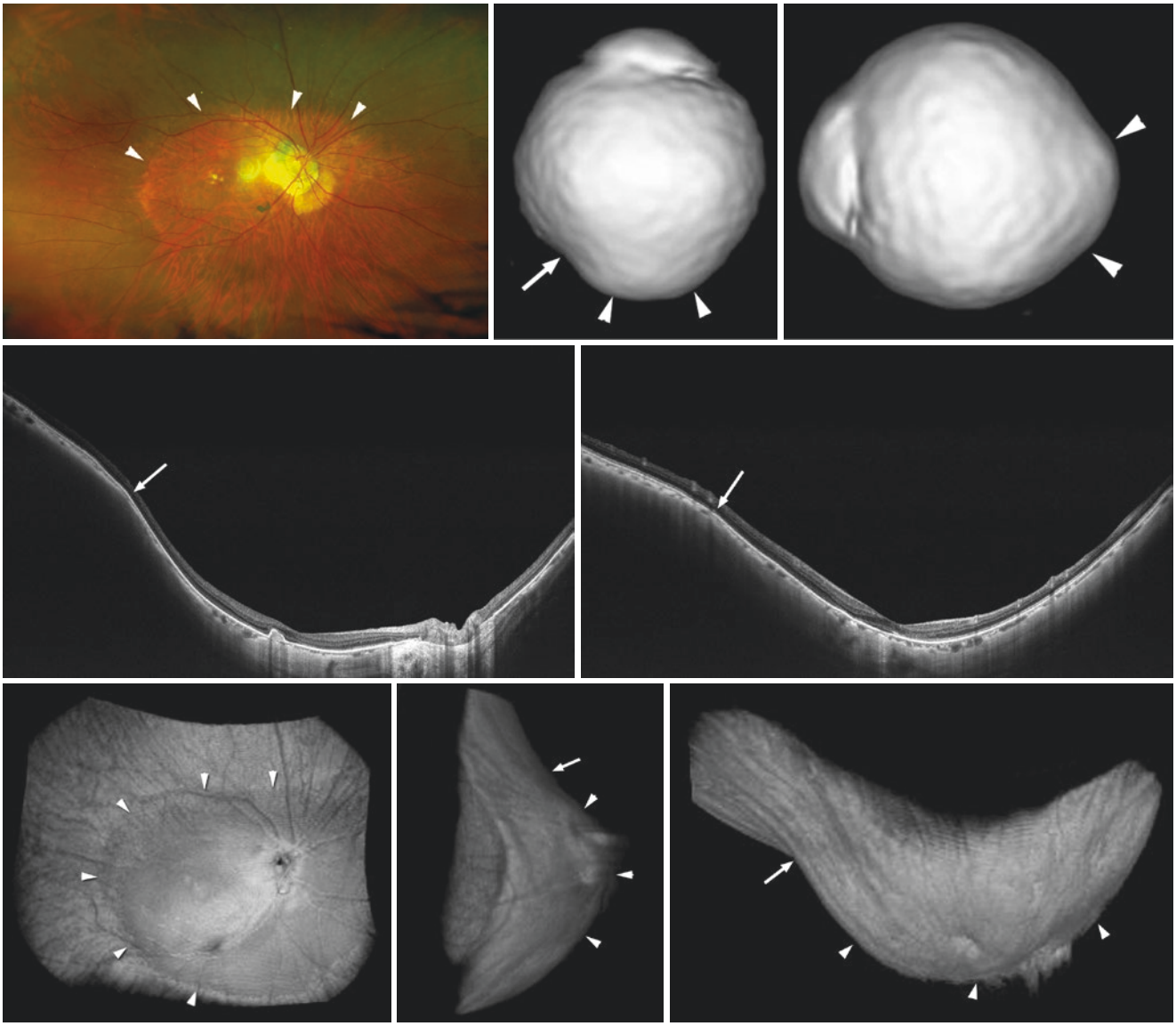

Fig. 5.1 Wide macular staphyloma as visualized by ultra-wide field optical coherence tomography (UWF-OCT) and three-dimensional magnetic resonance imaging (3D MRI). Cited with permission from [5]. Top left: Image of the right fundus of a 79-year-old woman (axial length: 26.6 mm) showing the border of a wide staphyloma as indicated by pigmentary abnormalities (arrowheads). Top middle and top right: 3D-MRI images viewed from the inferior (Middle) and from the nasal side (Right), showing a wide macular staphyloma (arrowheads) with a notch at the temporal border (arrow in Middle image). Middle row: Cross-sectional UWF-OCT images across the fovea. Left: horizontal scan. Right: vertical scan. An inward protrusion of the sclera and a thinning of the choroid are observed at the edge of the staphyloma in the horizontal section and in the vertical section (arrows). The staphylomatous region shows a posterior displacement of the sclera nasal to the staphyloma edge in the Left image and inferior to the staphyloma edge in the Right image. Bottom row: Three-dimensional UWF-OCT images viewed from the anterior (Left), the nasal (Middle), and from the inferior side (Right), show a scleral outpouching (arrowheads) due to a wide macular staphyloma. In the Left image, the staphyloma border is spatially associated with the optic nerve head and the retinal vessels

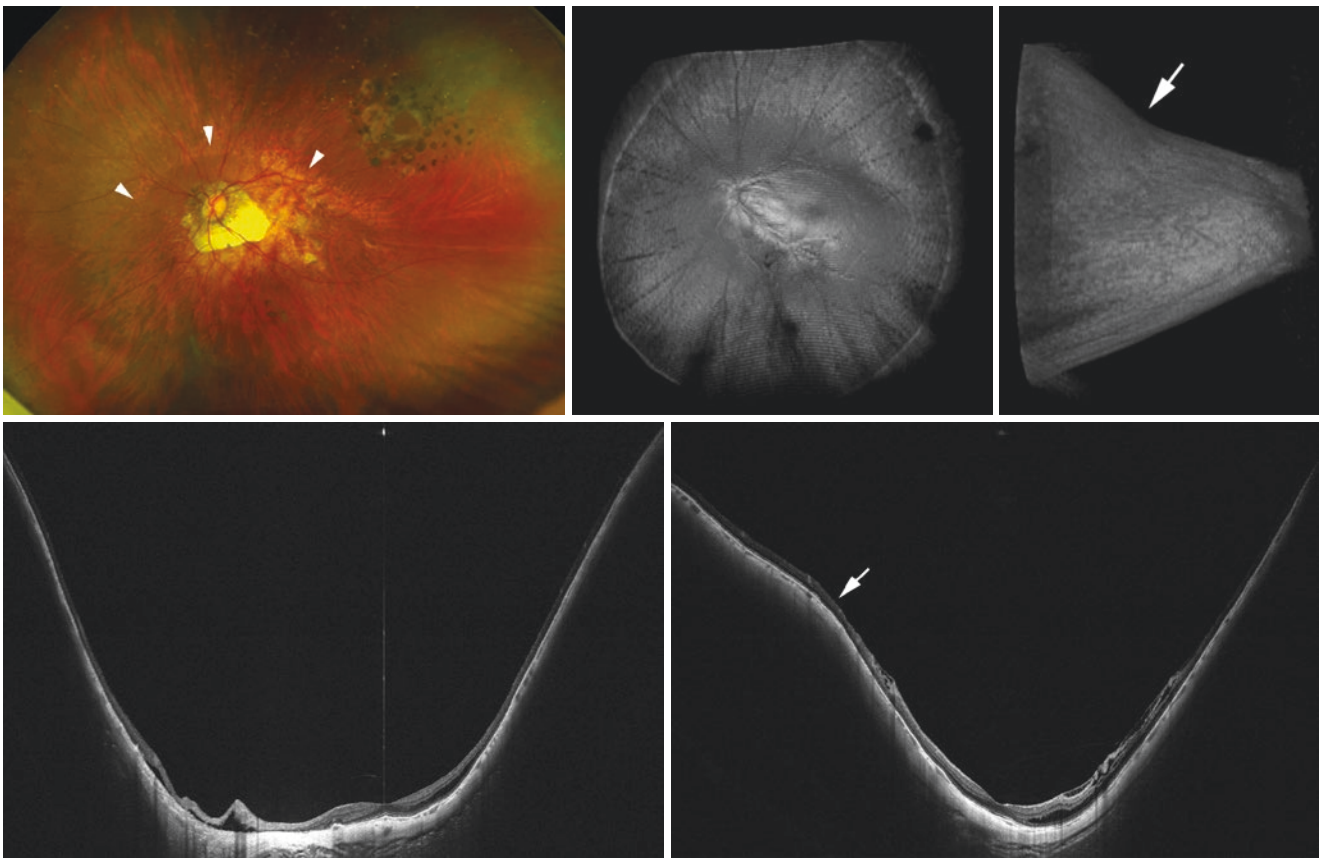

Fig. 5.2 Staphyloma classified as wide macular staphyloma by ultra-wide field optical coherence tomography (UWF-OCT). Top Left: Left fundus of a 56-year-old woman (length: 29.3 mm) showing the border of a wide macular staphyloma as indicated by pigmentary abnormalities (arrowheads). Top middle and Top right: 3D UWF-OCT images viewed from the anterior (Middle) and from the temporal side (Right) with a notch at the superior staphyloma edge (arrow). Bottom row: Cross-sectional UWF-OCT images across the fovea (Left: horizontal scan, Right: vertical scan) showing an inward protrusion of the sclera and a thinning of the choroid at the staphyloma edge in the vertical scan (Right image) (arrow). A posterior displacement of the sclera within the staphylomatous area inferior to the staphyloma edge in Right image is observed

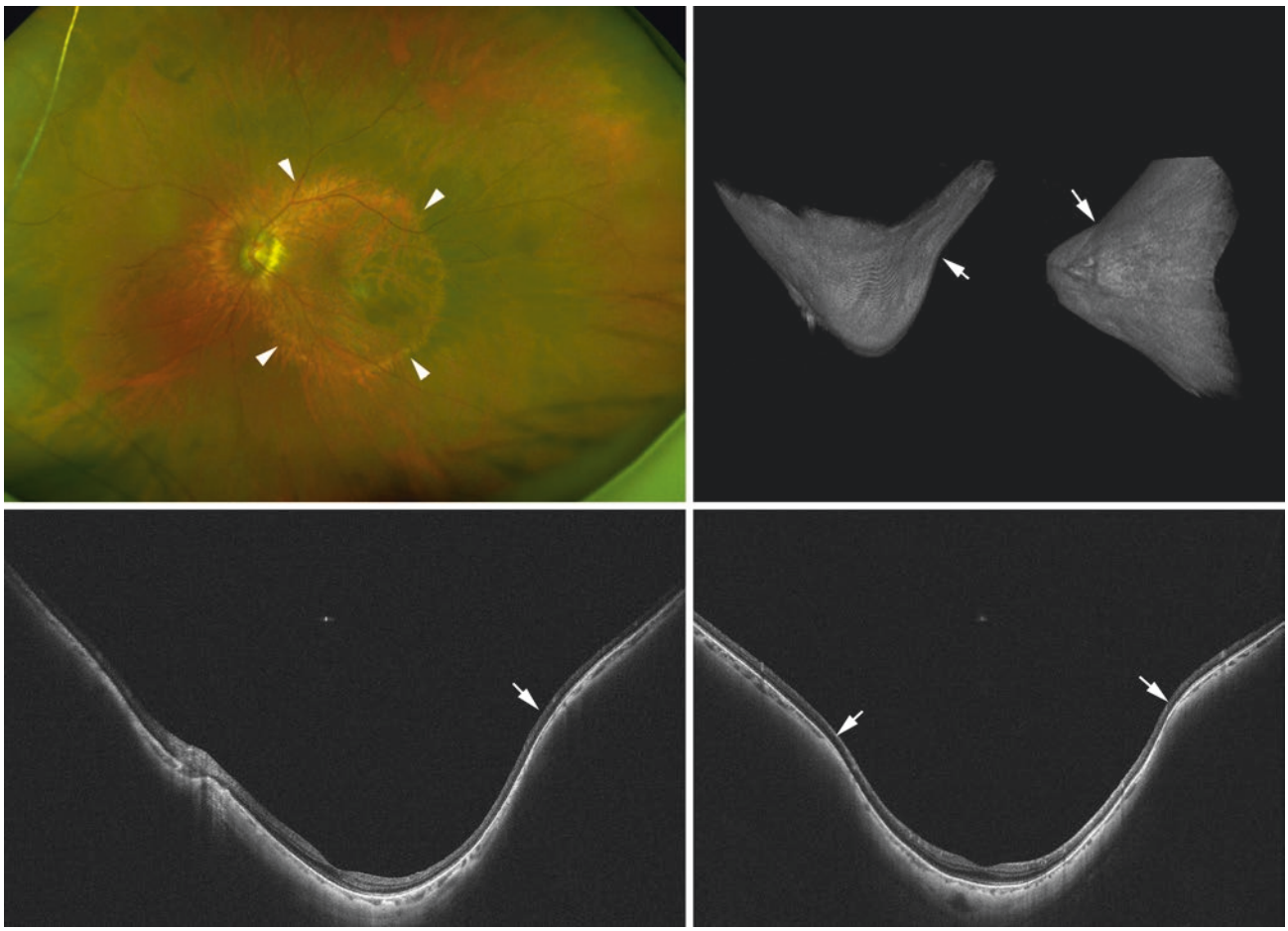

Fig. 5.3 Staphyloma classified as narrow macular staphyloma by ultra-wide field optical coherence tomography (UWF-OCT). Top Left: Left fundus of a 77-year-old woman (length: 26.6 mm) showing the border of a narrow macular staphyloma as indicated by pigmentary abnormalities (arrowheads). Top middle and Top right: 3D UWF-OCT images viewed from the inferior (Middle) and from the nasal side (Right) with a notch at the staphyloma edge (arrows). Bottom row: Cross-sectional UWF-OCT images across the fovea (Left: horizontal scan, Right: vertical scan) showing an inward protrusion of the sclera and a thinning of the choroid at the staphyloma edge (arrows). A posterior displacement of the sclera within the staphylomatous area is clearly observed

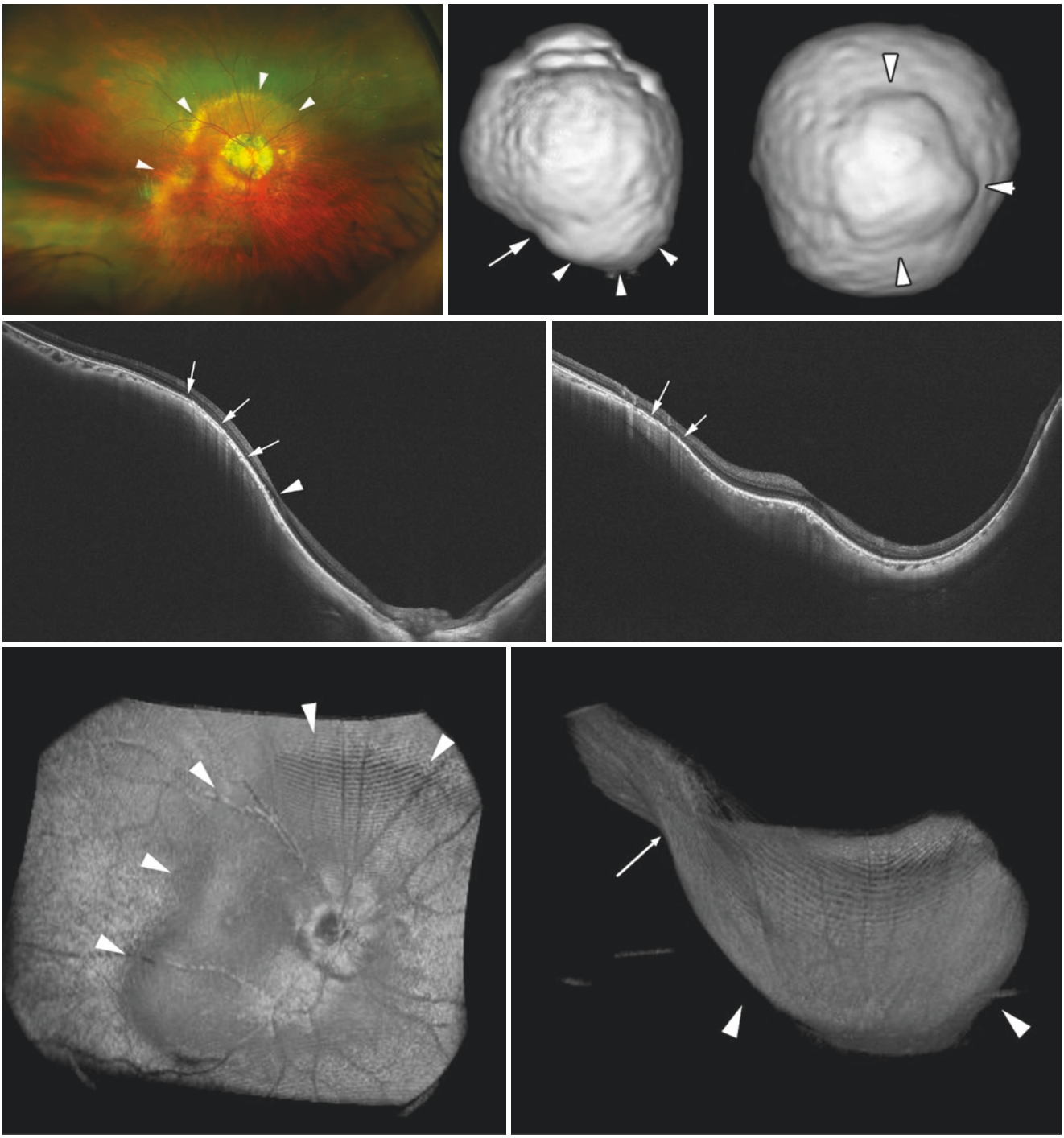

Fig. 5.4 Staphyloma classified as "others" (peripapillary and inferior type) both by three-dimensional magnetic resonance imaging (3D MRI) and ultra-wide field optical coherence tomography (UWF-OCT). Cited with permission from [5]. Top Left: Right fundus of a 68-year-old woman (axial length: 27.4 mm) with pigmentary abnormalities indicating the border of a staphyloma (arrowheads). Top Middle and Top Right: Three-dimensional magnetic resonance imaging (3D MRI) images viewed from the inferior (Middle) and from the posterior side (Right) showing a staphyloma (arrowheads). In the Middle image, the posterior outpouching is located mainly nasally; however, different from a peripapillary staphyloma, the outpouching has a wide opening angle. A notch is located at the temporal border of the staphyloma (arrow, Middle image). Due to the nasal dislocation of the wide scleral outpouching, this staphyloma type was classified as "others." Middle row: Cross-sectional UWF-OCT images across the fovea. Left: horizontal scan. Right: vertical scan. An inward protrusion of the sclera and a thinning of the choroid are located at the edge of the staphyloma both in the horizontal and vertical sections (arrows). A posterior displacement of the sclera is present in the staphylomatous area, nasal to the staphyloma edge in Left image and inferior to the staphyloma edge in Right image. The foveal region (arrowhead) is located on the slope of the staphyloma nasal to the staphyloma edge, and the optic nerve head is located at the bottom of the staphyloma in Left image. The Right image shows a posterior scleral displacement in the lower fundus with a dome-shaped appearance of the macula. This staphyloma was classified as "others" (peripapillary and inferior staphyloma type) by UWF-OCT. Bottom row: Three-dimensional UWF-OCT images viewed from the anterior (Left) and from the inferior side (Right) showing a peculiar shape of the staphyloma. The staphyloma is wider in the inferior fundus compared to the superior fundus. In the Left image, the spatial relationship between the optic nerve head and the retinal vessels is shown. The temporal border of the staphyloma is shown in the Right image (arrow)

Fig. 5.5 Early signs of posterior staphyloma in children. Cited with permission from [4]. Top Left: Left fundus of an 11-year-old girl with an axial length of 27.1 mm showing peripapillary diffuse atrophy. Top right: Horizontal ultra-wide field optical coherence tomography (UWF-OCT) image shows that the nasal choroid gradually thins toward the staphyloma edge (arrow) and gradually re-thickens toward the posterior pole (arrowheads). Inner scleral surface is posteriorly displaced in the area between the edge of the staphyloma (arrow) and nasal edge of the optic disc, compared to the curvature more nasal to the staphyloma edge. However, the scleral inward protrusion at staphyloma edge is not obvious. Bottom Left: Right fundus photograph of a 17-year-old young man with an axial length of 28.1 mm showing peripapillary diffuse chorioretinal atrophy (PDCA). Bottom right: Horizontal UWF-OCT image showing that the inner scleral surface is slightly displaced posteriorly nasal to the optic nerve. The choroid gradually thins toward the edge of the staphyloma (arrow) and re-thickens toward the posterior pole (yellow arrowheads). However, scleral inward protrusion at the staphyloma edge is not obvious. Choroidal thickening closer to the optic nerve appears to be similar to peripapillary intrachoroidal cavitation. In the area of the PDCA (blue arrowheads), the scleral curvature is also displaced posteriorly

Table 5.1 Correlation of types of posterior staphyloma identified by 3D MRI and wide-field OCT

OCT / 3D MRI	None	Wide macular	Narrow macular	Peripapillary	Nasal	Inferior	Others	Total
None	23	2	6	2	0	0	2	35
Wide macular	2	26	4	0	0	2	8	42
Narrow macular	0	0	17	0	0	0	0	17
Peripapillary	0	0	0	4	0	0	0	4
Nasal	0	0	0	0	0	0	0	0
Inferior	0	1	0	0	0	0	0	1
Others	0	0	0	0	0	0	1	1
Total	25	29	27	6	0	2	11	100

3D MRI three-dimensional magnetic resonance imaging, *OCT* optical coherence tomography
Number of observed agreements: 71 (71.0% of the observations)
Number of agreements expected by chance: 25.9 (25.89% of the observations)
Kappa = 0.609
SE of kappa = 0.058
95% confidence interval: From 0.496 to 0.722
The strength of agreement is considered to be "good"

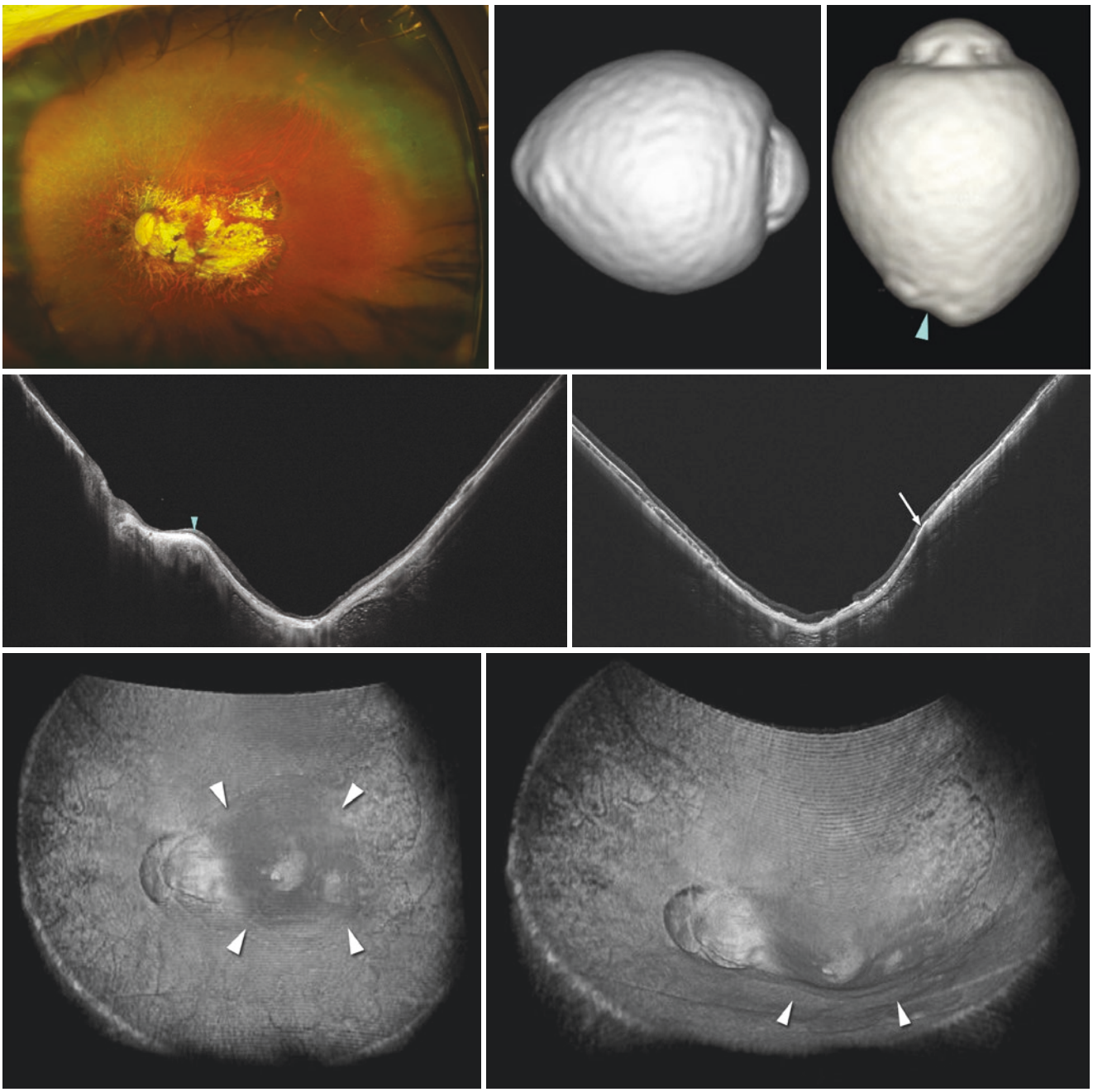

Fig. 5.6 An eye showing a narrow macular staphyloma by ultra-wide field optical coherence tomography (UWF-OCT) but no obvious protrusion by three-dimensional magnetic resonance imaging (3D MRI). Cited with permission from [5]. Top left: Left fundus of a 72-year-old woman (axial length: 31.6 mm) showing a severe chorioretinal atrophy and large parapapillary atrophy. Top Middle and Top Right: 3D-MRI images viewed from the nasal (Middle) and from the inferior side (Right). The eye is elongated without any obvious outpouching. A notch indicating the temporal ridge is observed (arrowhead in Right image). This case is classified as no staphyloma by 3D MRI. Middle row: Cross-sectional UWF-OCT images across the fovea. Left: horizontal scan. Right: vertical scan. An inward protrusion of the sclera and a thinning of the choroid are observed at the lower edge of the staphyloma in the vertical section (arrow, Right image). A posterior displacement of the sclera is shown within the staphylomatous area. The vertical ridge temporal to the optic nerve head is shown (arrowhead, Left image). Bottom row: Three-dimensional UWF-OCT images viewed from the anterior (Left) and from the anterior with slightly rotated angle (Right). The margin of the staphyloma is observed in both images (arrowheads). A spatial relationship between the staphylomatous area and the optic nerve head and the macula is demonstrated

References

1. Shinohara K, Moriyama M, Shimada N, Yoshida T, Ohno-Matsui K. Characteristics of Peripapillary Staphylomas associated with high myopia determined by swept-source optical coherence tomography. Am J Ophthalmol. 2016;169:138–44. https://doi.org/10.1016/j.ajo.2016.06.033.
2. Mori K, Kanno J, Gehlbach PL, Yoneya S. Montage images of spectral-domain optical coherence tomography in eyes with idiopathic macular holes. Ophthalmology. 2012;119(12):2600–8. https://doi.org/10.1016/j.ophtha.2012.06.027.
3. Uji A, Yoshimura N. Application of extended field imaging to optical coherence tomography. Ophthalmology. 2015;122(6):1272–4. https://doi.org/10.1016/j.ophtha.2014.12.035.
4. Tanaka N, Shinohara K, Yokoi T, Uramoto K, Takahashi H, Onishi Y, et al. Posterior staphylomas and scleral curvature in highly myopic children and adolescents investigated by ultra-widefield optical coherence tomography. PLoS One. 2019;14(6):e0218107. https://doi.org/10.1371/journal.pone.0218107.
5. Shinohara K, Shimada N, Moriyama M, Yoshida T, Jonas JB, Yoshimura N, et al. Posterior Staphylomas in pathologic myopia imaged by Widefield optical coherence tomography. Invest Ophthalmol Vis Sci. 2017;58(9):3750–8. https://doi.org/10.1167/iovs.17-22319.